ChemComm

Accepted Manuscript

This article can be cited before page numbers have been issued, to do this please use: T. F. Gronauer, M. M. Mandl, M. Lakemeyer, M. W. Hackl, M. Meßner, V. Korotkov, J. Pachmayr and S. A. Sieber, *Chem. Commun.*, 2018, DOI: 10.1039/C8CC05265D.

This is an Accepted Manuscript, which has been through the Royal Society of Chemistry peer review process and has been accepted for publication.

Accepted Manuscripts are published online shortly after acceptance, before technical editing, formatting and proof reading. Using this free service, authors can make their results available to the community, in citable form, before we publish the edited article. We will replace this Accepted Manuscript with the edited and formatted Advance Article as soon as it is available.

You can find more information about Accepted Manuscripts in the author guidelines.

Please note that technical editing may introduce minor changes to the text and/or graphics, which may alter content. The journal's standard Terms & Conditions and the ethical guidelines, outlined in our author and reviewer resource centre, still apply. In no event shall the Royal Society of Chemistry be held responsible for any errors or omissions in this Accepted Manuscript or any consequences arising from the use of any information it contains.

ROYAL SOCIETY OF CHEMISTRY

rsc.li/chemcomm

ChemComm

View Article Online
DOI: 10.1039/C8CC05265D

COMMUNICATION

Design and synthesis of tailored human caseinolytic protease P inhibitors†

Received 00th January 20xx,
Accepted 00th January 20xx

DOI: 10.1039/x0xx00000x

www.rsc.org/

Thomas F. Gronauer[a], Melanie M. Mandl[b], Markus Lakemeyer[a], Mathias W. Hackl[a], Martina Meßner[b], Vadim S. Korotkov[a], Johanna Pachmayr[b] and Stephan A. Sieber[a]*

Human caseinolytic protease P (hClpP) is important for degradation of misfolded proteins in the mitochondrial unfolded protein response. We here introduce tailored hClpP inhibitors that utilize a steric discrimination in their core naphthofuran scaffold to selectively address the human enzyme. This novel inhibitor generation exhibited superior activity compared to previously introduced beta-lactones, optimized for bacterial ClpP. Further insights into the bioactivity and binding to cellular targets were obtained via chemical proteomics as well as proliferation- and migration studies in cancer cells.

Mitochondria are essential for cellular energy production and represent a main source of reactive oxygen species (ROS).[1] Stress caused by ROS results in accumulation of damaged proteins which block essential functions and induce the mitochondrial unfolded protein response (mtUPR).[2] Human caseinolytic protease P (hClpP) represents a major mediator of cellular homeostasis in mtUPR by degradation of damaged proteins into peptides.[3,4] These peptides are transported across the inner mitochondrial membrane to activate stress-associated transcription factors.[5,6] hClpP is a serine protease expressed as inactive heptamers which assemble into an active tetradecamer by binding to hClpX.[7–9] Mice bearing a ClpP knockout suffer from hearing loss, infertility and growth defects. These effects are paralleled in humans by recessive mutations of hClpP causing the *Perrault* syndrome.[10] While hClpP is not essential for viability of normal cells, a recent study demonstrated its upregulation in patients with acute myeloid leukemia (AML).[11] Rapidly dividing cancer cells are exposed to multiple mitochondrial stresses and require an efficient UPR to maintain cell homeostasis. Accordingly, silencing of hClpP in AML cell lines increased mitochondrial ROS levels and thereby attenuated cell viability. hClpP thus represents a promising anti-

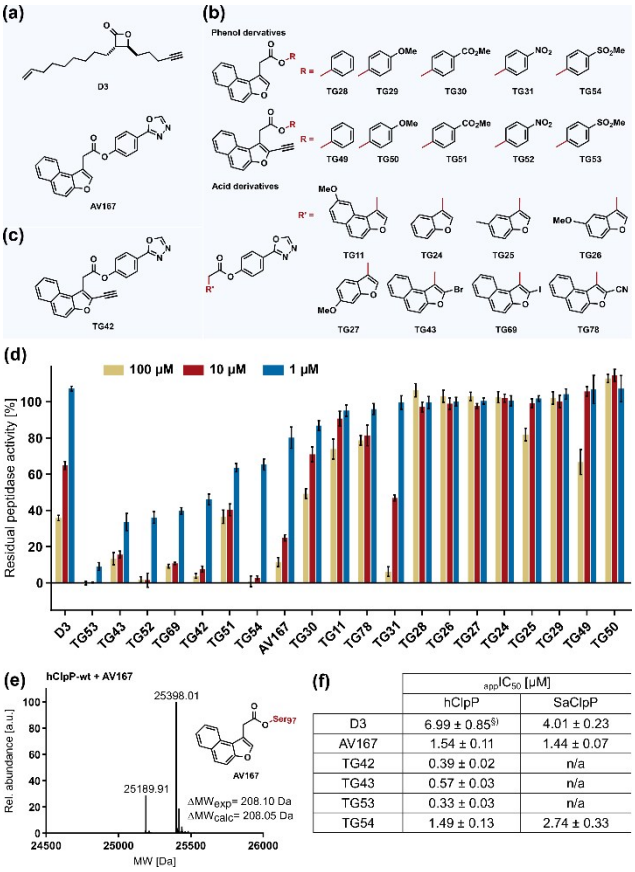

	$_{app}IC_{50}$ [µM]	
	hClpP	SaClpP
D3	6.99 ± 0.85§)	4.01 ± 0.23
AV167	1.54 ± 0.11	1.44 ± 0.07
TG42	0.39 ± 0.02	n/a
TG43	0.57 ± 0.03	n/a
TG53	0.33 ± 0.03	n/a
TG54	1.49 ± 0.13	2.74 ± 0.33

Fig. 1 (a) Structures of previous ClpP inhibitors: beta-lactone **D3** and phenyl ester **AV167**. (b) Structures of phenyl ester derivatives prepared in this study. (c) Structure of optimized probe **TG42** used for labeling. (d) hClpP peptidase activity assay (hClpP concentration 1 µM, fluorogenic substrate: Suc-L-Y-AMC (200 µM)). Experiments were carried out in six technical replicates from two independent experiments (mean ± standard deviation). (e) Intact protein mass spectrometry results showing high modification (78%) of hClpP by phenyl ester **AV167** (1 µM hClpP with 10-fold excess of **AV167**, 1 h incubation). (f) Results of apparent IC_{50} determination (§ 35% residual activity, see Fig. S3, ESI†).

[a] *Center for integrated Protein Science Munich, Department of Chemistry, Technische Universität München, Lichtenbergstraße 4, 85748 Garching, Germany*
* *E-mail: stephan.sieber@tum.de*
[b] *Paracelsus Medizinische Privatuniversität Salzburg, Strubergasse 21, 5020 Salzburg, Austria*

† Electronic Supplementary Information (ESI) available: Methods, Fig. S1-S7, Tables T1, T2, Schemes S1-S4, Table S1 (Excel file). Proteomic data are available *via* ProteomeXchange with identifier PXD010277. See DOI: 10.1039/x0xx00000x

View Article Online DOI: 10.1039/C8CC05265D

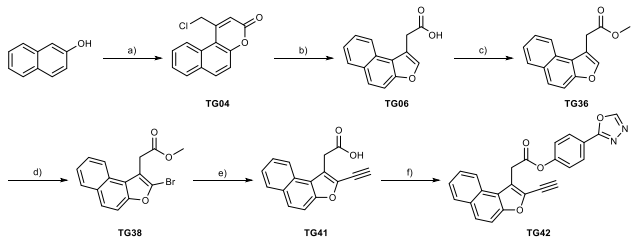

Scheme 1 Synthesis of compound **TG42**: (a) ethyl 4-chloroacetoacetate (1.14 eq.), H_2SO_4 (98%), 0 °C, 3 h, 92%; (b) 6 M $NaOH_{aq}$, 80 °C, 20 h, 96%; (c) H_2SO_4 (5.30 eq.), MeOH, 65 °C, 5 h, 91%; (d) NBS (1.09 eq.), $CHCl_3/CH_3CN$ (1:1), - 8 °C, 1 h, 90%; (e) 1. $Pd(PPh_3)_4$ (1.8 mol%), CuI (0.27 eq.), TMS-acetylene (2.00 eq.), NEt_3 (1.10 eq.), THF, rt, 20 h, 86%, 2. 1 M $LiOH_{aq}$, THF/H_2O (3:1), rt, 24 h, 93%; (f) EDC · HCl (1.50 eq.), DMAP (0.50 eq.), 1,3,4 oxadiazolyl phenol (**TG05**, 1.20 eq.), CH_2Cl_2, rt, 18 h, 49%.

cancer target.[12] Previous experiments with beta-lactone inhibitors, originally discovered and optimized for bacterial ClpPs,[13] induced death of leukemia cells and even reduced their growth in xenografted mice.[11] We recently discovered a next generation of bacterial ClpP inhibitors based on a phenyl ester scaffold.[14] Of note, one molecule, **AV167**, displayed superior inhibitory activity against hClpP exceeding that of previous beta-lactones (Fig. 1a).

We here systematically dissect the **AV167** core structure and identify novel inhibitors with superior potency for hClpP inhibition compared to the gold standard lactones. The inhibitors showed anti-proliferation, anti-migratory and apoptotic effects against cancer cells. Corresponding activity-based protein profiling (ABPP) suggested that multiple targets are likely responsible for these effects. Given the clinical need for novel hClpP inhibitors our scaffolds provide a unique starting point to further fine tune selectivity.

In a previous high-throughput screen against bacterial ClpP, **AV167**, bearing a characteristic naphthofuran moiety, protruded as the best hClpP inhibitor out of six phenyl ester hits.[14] We thus selected this scaffold for further optimization. First, covalent inhibition of hClpP was validated for **AV167** and compared to one of the best previous beta-lactone ClpP inhibitors (**D3**) (Fig. 1a). As quantitative acylation kinetics, represented in $k_{obs}/[I]$ values, could not be resolved for **AV167** due to its rapid binding velocity (data not shown), we performed two alternative assays assessing the reactivity and potency. ClpP inhibitors have been previously characterized by their inhibition of ClpP peptidase activity at three different concentrations (100, 10 and 1 µM).[14–16] **AV167** significantly reduced hClpP turnover already at 10 µM and intact mass-spectrometric (MS) analysis of the modified enzyme revealed about 80 % binding (Fig. 1d, e, S1, ESI†). Contrary, **D3** only achieved 65 % inhibition at the highest concentration tested (Fig. 1d). This trend is also reflected by corresponding apparent IC_{50} values determined at identical incubation times. **D3** displayed a 4.5-fold higher value compared to **AV167** and again retained 35 % residual enzyme activity at saturating concentrations indicating restricted binding (Fig. 1f, S3, ESI†). Based on these promising properties, **AV167** was selected for structure-activity relationship (SAR) studies to i) dissect the structure for essential enzyme recognition motifs and ii) identify possible sites for functionalization with a benign tag for target identification via ABPP.[17–19] Synthesis of five derivatives bearing an 8-methoxynaphthofuran moiety (**TG11**) or different substituted benzofurans (**TG24**-**TG27**) resulted in inactive compounds (Fig. 1b, Scheme S1, ESI†). Thus, modifications at a different site were subsequently explored by introducing a bromine substituent (**TG43**) and an alkyne tag at 2-position (**TG42**) (Fig. 1b, c, Scheme 1). Synthesis of these derivatives started with Pechmann reaction of 2-naphthol and ethyl 4-chloroacetoacetate to the corresponding β-naphthocoumarin (**TG04**) which rearranged under basic conditions to naphthofuranylacetic acid (**TG06**). Ester protection and subsequent electrophilic bromination with NBS led to the precursor (**TG38**) for Sonogashira coupling with TMS-protected acetylene. Deprotection of the carboxylic ester and TMS-protecting group could be achieved in one step with aqueous LiOH solution. Esterification with oxadiazolyl phenol (**TG05**), derived from methyl paraben via two step synthesis, resulted in compound **TG42** (Scheme 1). Satisfyingly, probe **TG42** and its bromo precursor **TG43** exhibited elevated potency compared to **AV167** (1.54 µM) with apparent IC_{50}s of 0.39 and 0.57 µM, respectively (Fig. 1b, f, S3, ESI†). Intact MS revealed about 50 % modification to be sufficient to achieve full inhibition (Fig. S1, ESI†). As **AV167** bears an activated ester moiety we systematically tested the inhibition profiles of various ester derivatives (Fig. 1b, d). As expected alcohols exhibiting electron-donating properties such as phenol and *p*-methoxyphenol (**TG28**, **TG29**) turned out to be poor inhibitors while derivatives with electron withdrawing groups including *p*-nitro- and *p*-methylsulfonylphenol (**TG30**, **TG51**, **TG52**, **TG54**) showed inhibition profiles comparable to the parent *p*-oxadiazolylphenol of **AV167**. All compounds with activated ester moieties and naphthofuran substituents in 2-position (**TG42**, **TG43**, **TG53**) displayed potent IC_{50}s ranging from 0.33 - 0.57 µM, indicating sub-stoichiometric inhibition of hClpP (used at 1 µM in this assay) (Fig. 1f, Scheme S1-S5, ESI†). Contrary to **AV167**, these compounds showed only minor inhibition of *S. aureus* ClpP, demonstrating a crucial discrimination of species selectivity caused by substituents attached to the naphthofuran ring at 2-position (Fig. 1f, S2, ESI†).

To assess the ability of these compounds to block proteolytic activity hClpP was activated via an acyldepsipeptide derived chaperone mimic.[20,21] Binding of this activator fragment to hydrophobic pockets induces pore opening and digest of FITC casein. While beta-lactone **D3** showed no activity, **AV167**, **TG42** and **TG52**-**TG54** efficiently blocked proteolysis (Fig. 2a). This result was further corroborated by a second proteolysis assay in presence of the ClpX chaperone.[22,23] *Escherichia coli* ClpX (EcClpX) forms a functionally active complex with hClpP and is preferred in these assays compared to the largely uncharacterized human ClpX.[7] For enzyme activity assessment, degradation of green fluorescent protein (GFP) tagged with an EcClpX recognition sequence was monitored.[23] All new derivatives exhibited strong inhibition down to 1 µM concentration (Fig. 2b), a remarkable result given the previous difficulties of chemical inhibitors to overcome conformational

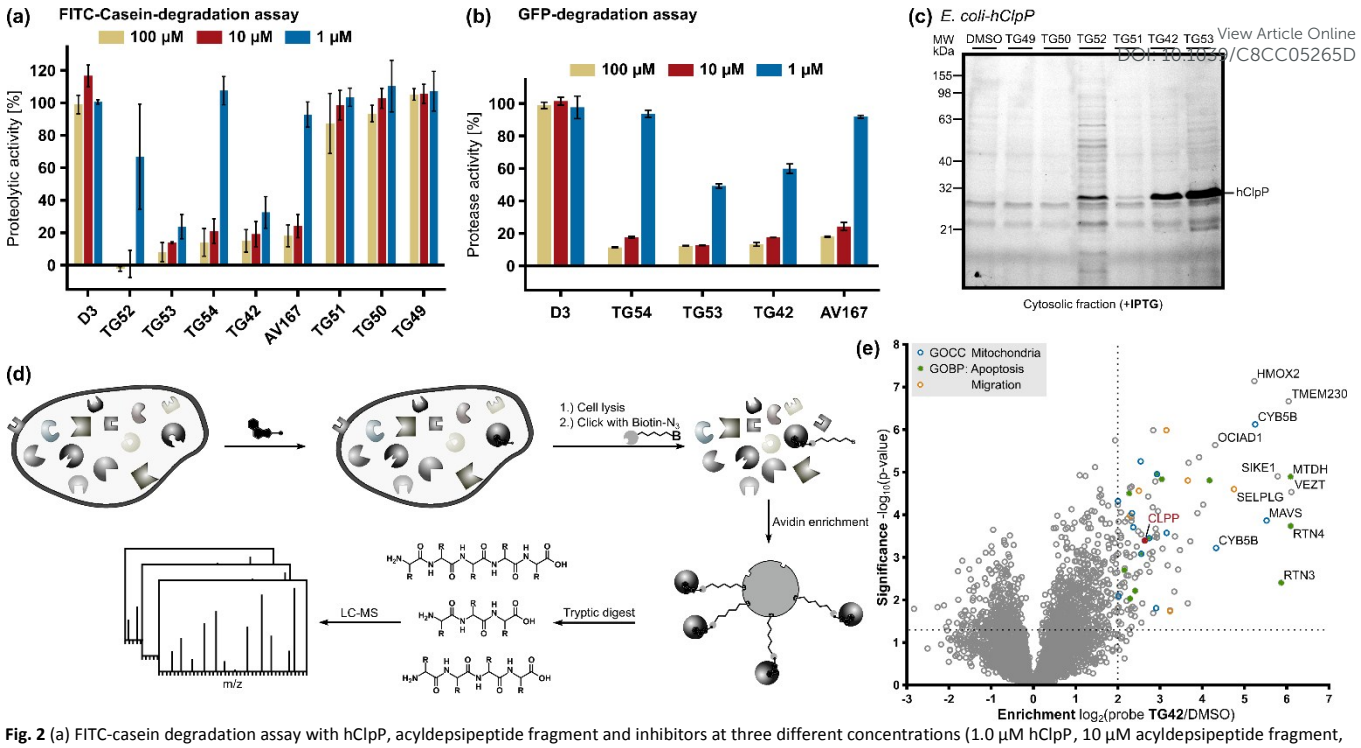

Fig. 2 (a) FITC-casein degradation assay with hClpP, acyldepsipeptide fragment and inhibitors at three different concentrations (1.0 µM hClpP, 10 µM acyldepsipeptide fragment, 2 µM FITC-casein. Each data-set represents results from six replicates obtained from two independent experiments. (b) hClpP GFP protease assay (0.2 µM hClpP in the presence of 0.4 µM EcClpX and 0.4 µM GFP-SsrA) with compounds as indicated. Each data-set represents results from three replicates (mean ± standard deviation) (c) ABPP-labeling of recombinantly expressed hClpP in *E. coli* Rosetta2 expression strains. SDS-PAGE of soluble fraction shows distinct bands at ≈ 32 kDa. For Coomassie stained SDS-PAGE gels see Fig. S7 ESI†. (d) Schematic representation of the ABPP workflow: Cells are incubated with electrophilic compounds which react with reactive amino acids of target proteins. Following cell lysis, click reaction to affinity tag bitoin-N_3 and enrichment on avidin beads, proteins are tryptically digested and analyzed by LC-MS/MS. (e) Volcano plot representation of gel-free quantitative ABPP experiment with **TG42** in Jurkat cells (20 µM **TG42**, 1 h labeling) depicting enrichment and significance of enrichment from four technical replicates. Color codes show connection to certain cell compartment (GOCC) and biological processes (GOBP) by gene ontology analysis. Two sample student's t-test was performed by comparison of labeled group against DMSO as single control group with Benjamini-Hochberg FDR correction set to 0.05. Cut-off lines were set at a minimum $\log_2$ change of 2 and a minimum p-value of 0.05.

rearrangements within ClpP upon chaperone or small molecule activator binding.[22] Reactivity and selectivity of all alkynylated compounds was tested against recombinant hClpP expressed in *E. coli* cells. Intact cells were incubated with the probes, lysed, clicked to rhodamine azide[24,25] and analyzed via fluorescent SDS-PAGE. hClpP was clearly labeled by **TG42**, **TG52** and **TG53** with **TG42** bearing the best signal to noise ratio (Fig. 2c). As hClpP is located in mitochondria, a specific inhibitor needs to permeate two membrane barriers for target engagement. To test if **TG42** is able to address mitochondrial hClpP in living cancer cells, we performed a gel-free whole proteome LC-MS/MS analysis (Fig. 2d). For this intact Jurkat and Huh7 cells, shown to express hClpP by western blot (Fig. S4, ESI†), were incubated with the probes, lysed, clicked to biotin azide,[24,25] enriched via binding to avidin beads and finally released by tryptic digest.[14] In parallel the same procedure was carried out with DMSO-treated cells as control. Peptides were subjected to high-resolution LC-MS/MS and multiple biological replicates were analyzed via label-free quantification (Fig. 2d).[26] **TG42** significantly enriched hClpP in Jurkat cells, however, a large number of other prominent targets were additionally obtained, suggesting that the electrophilic probe is of either limited selectivity in human proteomes or has restricted access to mitochondrial compartments (Fig. 2e, S5, ESI†). In contrast, labeling of Huh7 cells (Fig. S6, ESI†) and Jurkat cells[27] with lactone **D3** resulted in no enrichment of hClpP at all. Thus, despite its superior in vitro potency and labeling performance compared to previous inhibitors, further optimization of **TG42** is required to enhance cellular selectivity for mitochondrial hClpP. Nevertheless, given the crucial role of hClpP and several of the identified targets such as Reticulon[28] and Protein LYRIC[29] in apoptosis (Fig. 2e, S5, ESI†) we investigated the biological consequences of **TG42** in Huh7 cancer cells and demonstrated concentration-dependent cell death with induction of apoptosis (Fig. 3a, b). Cancer cell migration could also be significantly reduced at 30 µM **TG42** treatment (Fig. 3c).

Selective eradication of cancer cells is an important task in drug development to reduce side effects of chemotherapy. hClpP is a promising target in this endeavor lacking inhibitors for therapeutic applications. **AV167** represented a starting point to achieve this goal bearing a characteristic curved naphthofuran moiety suitable to durably inhibit ClpP peptidolytic as well as proteolytic activities. Importantly, substitution at 2-position of the naphthofuran moiety not only enhanced *in vitro* potency but also represented a crucial signature motif differentiating between binding into human or bacterial ClpP isoforms. **TG42** exhibited superior inhibition and selectivity towards hClpP compared to a reference beta-lactone. Further fine-tuning of the inhibitor scaffold is needed to enhance its cellular selectivity.

This work was supported by the Deutsche Forschungsgemeinschaft SI1096/8-1 (ClpP) and CIPSM.

View Article Online
DOI: 10.1039/C8CC05265D

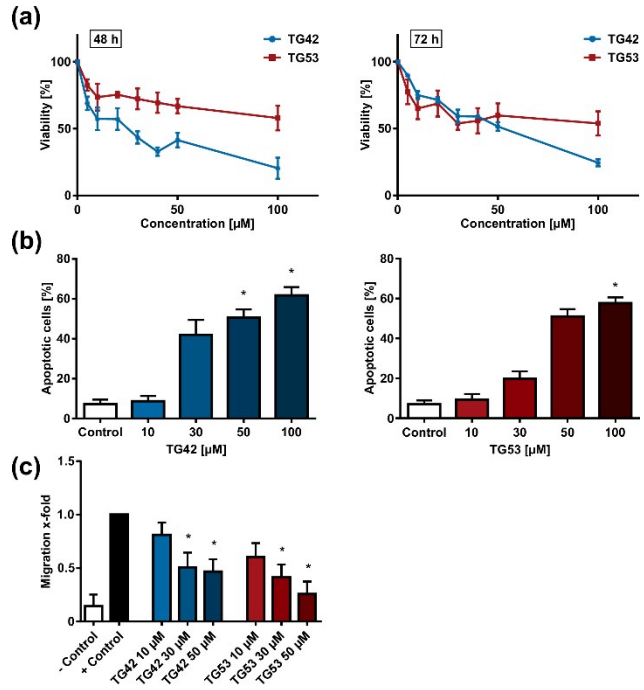

Fig. 3 (a) hClpP inhibitors reduce cell viability in Huh7 cells after treatment for 48 h and 72 h (CellTiterBlue® assay). Diagrams depict results of nine technical replicates from three independent experiments (mean ± standard deviation). (b) ClpP inhibitors **TG42** and **TG53** induce apoptotic cell death in Huh7 cells after 42 h treatment. Apoptosis was measured by flow cytometry using Nicoletti Assay (cell permeabilization, propidium iodide staining, gating of subG1 population, * p<0.05, mean ± SEM, one-way ANOVA, Tukey's Multiple Comparison, n=3). (c) hClpP inhibitors decrease Huh7 cell migration after incubation for 16 h with **TG42** and **TG53**, respectively (mean ± SEM, * p<0.05, One-way ANOVA, Dunnet's test, n=3).

Conflicts of interest

There are no conflicts to declare.

Notes and references

1 M. P. Murphy, *Biochem. J.*, 2009, **417**, 1–13.
2 V. Jovaisaite, L. Mouchiroud and J. Auwerx, *J. Exp. Biol.*, 2014, **217**, 137–143.
3 M. P. L. Gibellini, S. De Biasi, M. Nasi, A. Iannone, A. Cossarizza, *Curr. Pharm. Des.*, 2016, **22**, 2679–2688.
4 C. A. Goard and A. D. Schimmer, *Oncogene*, 2014, **33**, 2690–2699.
5 C. M. Haynes, K. Petrova, C. Benedetti, Y. Yang and D. Ron, *Dev. Cell*, 2007, **13**, 467–480.
6 C. M. Haynes, Y. Yang, S. P. Blais, T. A. Neubert and D. Ron, *Mol. Cell*, 2010, **37**, 529–540.
7 S. G. Kang, J. Ortega, S. K. Singh, N. Wang, N. Huang, A. C. Steven and M. R. Maurizi, *J. Biol. Chem.*, 2002, **277**, 21095–21102.
8 K. N. Truscott, A. Bezawork-Geleta and D. A. Dougan, *IUBMB Life*, 2011, **63**, 955–963.
9 S. G. Kang, M. N. Dimitrova, J. Ortega, A. Ginsburg and M. R. Maurizi, *J. Biol. Chem.*, 2005, **280**, 35424–35432.
10 S. Gispert, D. Parganlija, M. Klinkenberg, S. Dröse, I. Wittig, M. Mittelbronn, P. Grzmil, S. Koob, A. Hamann, M. Walter, F. Büchel, T. Adler, M. Hrabé de Angelis, D. H. Busch, A. Zell, A. S. Reichert, U. Brandt, H. D. Osiewacz, M. Jendrach and G. Auburger, *Hum. Mol. Genet.*, 2013, **22**, 4871–4887.
11 A. Cole, Z. Wang, E. Coyaud, V. Voisin, M. Gronda, Y. Jitkova, R. Mattson, R. Hurren, S. Babovic, N. Maclean, I. Restall, X. Wang, D. V. Jeyaraju, M. A. Sukhai, S. Prabha, S. Bashir, A. Ramakrishnan, E. Leung, Y. H. Qia, N. Zhang, K. R. Combes, T. Ketela, F. Lin, W. A. Houry, A. Aman, R. Al-awar, W. Zheng, E. Wienholds, C. J. Xu, J. Dick, J. C. Y. Wang, J. Moffat, M. D. Minden, C. J. Eaves, G. D. Bader, Z. Hao, S. M. Kornblau, B. Raught and A. D. Schimmer, *Cancer Cell*, 2015, **27**, 864–876.
12 V. Bhandari, K. S. Wong, J. L. Zhou, M. F. Mabanglo, R. A. Batey and W. A. Houry, *ACS Chem. Biol.*, 2018, **13**, 1413-1425.
13 T. Bottcher and S. a Sieber, *J. Am. Chem. Soc.*, 2008, **130**, 14400–14401.
14 M. W. Hackl, M. Lakemeyer, M. Dahmen, M. Glaser, A. Pahl, K. Lorenz-Baath, T. Menzel, S. Sievers, T. Böttcher, I. Antes, H. Waldmann and S. A. Sieber, *J. Am. Chem. Soc.*, 2015, **137**, 8475–8483.
15 M. Gersch, F. Gut, V. S. Korotkov, J. Lehmann, T. Böttcher, M. Rusch, C. Hedberg, H. Waldmann, G. Klebe and S. A. Sieber, *Angew. Chemie - Int. Ed.*, 2013, **52**, 3009–3014.
16 F. Weinandy, K. Lorenz-Baath, V. S. Korotkov, T. Böttcher, S. Sethi, T. Chakraborty and S. A. Sieber, *ChemMedChem*, 2014, **9**, 710–713.
17 M. J. Evans and B. F. Cravatt, *Chem. Rev.*, 2006, **106**, 3279–3301.
18 M. Fonović and M. Bogyo, *Expert Rev. Proteomics*, 2008, **5**, 721–730.
19 W. P. Heal, T. H. T. Dang and E. W. Tate, *Chem. Soc. Rev.*, 2011, **40**, 246–257.
20 D. W. Carney, C. L. Compton, K. R. Schmitz, J. P. Stevens, R. T. Sauer and J. K. Sello, *Chembiochem*, 2014, **15**, 2216–2220.
21 H. Brötz-Oesterhelt, D. Beyer, H. P. Kroll, R. Endermann, C. Ladel, W. Schroeder, B. Hinzen, S. Raddatz, H. Paulsen, K. Henninger, J. E. Bandow, H. G. Sahl and H. Labischinski, *Nat. Med.*, 2005, **11**, 1082–1087.
22 A. Pahl, M. Lakemeyer, M. T. Vielberg, M. W. Hackl, J. Vomacka, V. S. Korotkov, M. L. Stein, C. Fetzer, K. Lorenz-Baath, K. Richter, H. Waldmann, M. Groll and S. A. Sieber, *Angew. Chemie - Int. Ed.*, 2015, **54**, 15892–15896.
23 Y. I. Kim, R. E. Burton, B. M. Burton, R. T. Sauer and T. A. Baker, *Mol. Cell*, 2000, **5**, 639–648.
24 V. V. Rostovtsev, L. G. Green, V. V. Fokin and K. B. Sharpless, *Angew. Chem. Int. Ed.*, 2002, **41**, 2596–2599.
25 C. W. Tornøe, C. Christensen and M. Meldal, *J. Org. Chem.*, 2002, **67**, 3057–3064.
26 E. C. Keilhauer, M. Y. Hein and M. Mann, *Mol. Cell. Proteomics*, 2015, **14**, 120–135.
27 M. H. Wright, Y. Tao, J. Drechsel, J. Krysiak, S. Chamni, A. Weigert-Munoz, N. L. Harvey, D. Romo and S. A. Sieber, *Chem. Commun.*, 2017, **53**, 12818–12821.
28 Q. Wan, E. Kuang, W. Dong, S. Zhou, H. Xu, Y. Qi and Y. Liu, *Apoptosis*, 2007, **12**, 319–328.
29 L. Emdad, S. K. Das, B. Hu, T. Kegelman, D. C. Kang, S. G. Lee, D. Sarkar and P. B. Fisher, *Adv. Cancer Res.*, 2016, **131**, 97–132.

View Article Online
DOI: 10.1039/C8CC05265D

Table of contents

To expedite functional studies of human ClpP we introduce tailored small molecule inhibitors. These compounds are active against the proteolytic ClpXP complex. Target identification elucidates anti-proliferative effects against cancer cells.